HHS Public Access

Author manuscript

Cancer Lett. Author manuscript; available in PMC 2018 August 01.

Published in final edited form as:

Cancer Lett. 2017 August 01; 400: 110–116. doi:10.1016/j.canlet.2017.04.019.

The dual mTOR kinase inhibitor TAK228 inhibits tumorigenicity and enhances radiosensitization in diffuse intrinsic pontine glioma

Hiroaki Miyahara[a], **Sridevi Yadavilli**[b], **Manabu Natsumeda**[a], **Jeffrey Rubens**[c], **Louis Rodgers**[d], **Madhuri Kambhampati**[b], **Isabella Taylor**[c], **Harpreet Kaur**[c], **Laura Asnaghi**[a], **Charles G. Eberhart**[a], **Katherine E. Warren**[d], **Javad Nazarian**[b,e], and **Eric H. Raabe**[a,c]

[a]Department of Pathology, Division of Neuropathology, Johns Hopkins University School of Medicine, Baltimore, MD. USA

[b]Research Center for Genetic Medicine, Children's National Health System, Washington, District Of Columbia 20010, USA

[c]Division of Pediatric Oncology, Sidney Kimmel Comprehensive Cancer Center, Johns Hopkins University School of Medicine, Baltimore, MD. USA

[d]National Cancer Institute, National Institute of Health, Bethesda, Maryland 20892, USA

[e]Department of Integrative Systems Biology, George Washington University School of Medicine and Health Sciences, Washington, District Of Columbia 20052, USA

Abstract

Diffuse intrinsic pontine glioma (DIPG) is an invasive and treatment-refractory pediatric brain tumor. Primary DIPG tumors harbor a number of mutations including alterations in *PTEN, AKT*and *PI3K* and exhibit activation of mammalian Target of Rapamycin Complex 1 and 2 (mTORC1/2). mTORC1/2 regulate protein translation, cell growth, survival, invasion, and metabolism. Pharmacological inhibition of mTORC1 is minimally effective in DIPG. However, the activity of dual TORC kinase inhibitors has not been examined in this tumor type.

Nanomolar levels of the mTORC1/2 inhibitor TAK228 reduced expression of p-AKT^{S473} and p-S6$^{S240/244}$ and suppressed the growth of DIPG lines JHH-DIPG1, SF7761, and SU-DIPG-XIII. TAK228 induced apoptosis in DIPG cells and cooperated with radiation to further block proliferation and enhance apoptosis.

TAK228 monotherapy inhibited the tumorigenicity of a murine orthotopic model of DIPG, more than doubling median survival (p=0.0017) versus vehicle. We conclude that dual mTOR inhibition is a promising potential candidate for DIPG treatment.

Corresponding Author: Eric H Raabe, MD, PhD, Johns Hopkins University School of Medicine, Bloomberg 11379, 1800 Orleans, Baltimore, MD 21287, USA eraabe2@jhmi.edu.

Conflict of interest statement. Authors declare no conflict of interest.

Keywords

pediatric brain tumor; sapanisertib; mTOR; INK128; MLN0128

1. Introduction

Diffuse intrinsic pontine glioma (DIPG) is an invasive, treatment-refractory brain tumor mainly occurring in children. Despite aggressive treatment, the majority of patients die within 2 years after initial diagnosis [1]. Recent studies have identified mutations in histone genes (*H3F3A, HIST1H3B, HIST2H3C*) encoding histone H3.3, H3.1 and H3.2 (H3K27M) proteins [2; 3; 4; 5; 6; 7], *TP53* mutation [5], activating receptor *ACVR1* mutation [8], AKT gain, and PTEN loss [9; 10; 11].

The mammalian Target of Rapamycin (mTOR) signaling pathway is one of the key oncogenic signaling pathways. mTOR Complex 1 (mTORC1) is an upstream activator of S6 and 4E-BP1, and regulates protein synthesis, lipid synthesis, energy metabolism, autophagy, lysosome function, and maintains cell homeostasis [12]. The known functions of mTORC2 include apoptosis prevention [13], metabolic control, and actin polarization [14]. Approximately 70% of DIPG tumors have either AKT gain or PTEN loss, suggesting frequent aberrations of PTEN/AKT/mTOR signaling pathway in this disease [9; 15].

Targeting mTOR has largely relied on agents such as rapamycin and everolimus, which primarily inhibit mTORC1 by allosteric binding [16]. A screen of these drugs against DIPG cells showed that they were ineffective [17]. Inhibition of mTORC1 by these agents often leads to upregulation of mTORC2, which may contribute to the relative lack of effectiveness of mTORC1 inhibitors [18]. New dual mTORC kinase inhibitors may have broader therapeutic use than rapalogs, due to their ability to inhibit both mTORC1 and mTORC2 [19].

TAK228, also known as sapanisertib, MLN0128 and INK128, is an ATP-competitive mTOR kinase inhibitor that inhibits both TORC1 and TORC2 [20; 21]. TAK228 has been found to be active in solid tumors such as sarcoma [22], pancreatic cancer [23], neuroblastoma [24], and breast cancer [21; 25]. There are two ongoing clinical trials (NCT02133183, NCT02142803) using TAK228 in adult glioblastoma, evaluating its ability to penetrate the brain and suppress mTORC1/2. No pediatric brain tumor clinical studies have been conducted with TAK228 to date.

Because most DIPG have genetic aberrations in the PI3K/AKT/mTOR pathway, we hypothesized that TAK228 would be effective in this tumor type. Herein, we evaluated the effects of dual TAK228 in DIPG and found that it suppressed cell growth, proliferation, invasion, induced apoptosis and more than doubled the median survival of an orthotopic murine model of DIPG.

2. Materials and Methods

2.1 Cell culture conditions and drug preparation

JHH-DIPG1, SF7761, and SU-DIPG-XIII DIPG neurosphere lines were maintained in DMEM/F12 medium supplemented with 20 ng/ml epidermal growth factors (EGF) and 20 ng/ml fibroblast growth factors (FGF) (EF media) [26]. To avoid differentiation of SU-DIPG-XIII cells, EF media without retinoic acid was used [17]. The JHH-DIPG1 line was derived from a rapid autopsy specimen and established in our laboratory as previously described [26]. The SF7761 line is a kind gift from Rintaro Hashizume and Nalin Gupta (University of California, San Francisco, CA) [27], and the SU-DIPG-XIII line is a kind gift of Michelle Monje (Stanford University School of Medicine, Stanford, CA) [28]. All DIPG lines were verified to be mycoplasma-free by polymerase chain reaction (PCR) testing. Authentication of the DIPG cell lines was performed using short tandem repeat (STR) profiling by the Johns Hopkins Genetic Resources Core Facility. For treatment studies, these neurospheres were disassociated into single cells using Accutase (Sigma-Aldrich, St Louis, MO), counted, plated, and allowed to grow for 3 days in EF media before administration of drugs. Then, dimethyl sulfoxide (DMSO, vehicle control; Sigma-Aldrich) or 1–125 nM TAK228 dissolved in DMSO was added into the cell-containing medium. PKC (PDGFB/H3.3-K27M/p53−/−) murine cells and luciferase-expressing PKC-L [29] were grown in NeuroCult mouse basal media supplemented with 10% mouse cell proliferation supplement (Stem cell technologies), glutamine, penicillin-streptomycin, heparin (2 μg/μl), rm EGF (20 ng/mL) and rm FGF (20 ng/mL). Cultures were maintained at 5% CO2 at 37°C. For *in vitro* viability assays, 10,000 cells in triplicates for each condition were seeded in 96 well plates on day 1. On day 2 cells were treated with TAK228. On day 7, viability was assessed using CytoTox-Glo cytotoxicity assay (Promega).

2.2 Western blot analysis

The treated cells and xenografts were lysed in RIPA buffer containing protease inhibitor cocktail (Sigma-Aldrich) and phosphatase inhibitors and western blotting was performed as described previously [30]. Membranes were then probed with primary antibodies overnight. The following primary antibodies were used: phosphorylated AKT at Ser473 (p-AKT^{S473}), AKT (C6E7), S6 (54D2), cleaved PARP (D214) (D64E10), BCL-2 (15071S), BCL-XL (2764S) (1:1,000 dilution, Cell Signaling Technology, Danvers, MA), phosphorylated S6 at Ser240/244 (p-S6$^{S240/244}$; 1:2,000 dilution, Cell Signaling, Danvers, MA), and β-ACTIN (C4) (1:2,000 dilution, Sigma-Aldrich). Secondary antibodies conjugated to horseradish peroxidase (1:2,000 dilution, KPL, Gaithersburg, MD) were incubated for 1 hour and detected with a Western Lightning Plus ECL chemiluminescence kit (PerkinElmer, Waltham, MA). Densitometry was performed using Image J Ver. 1.440 software (http://rsb.info.nih.gov/ij/)[31].

2.3 Cell growth assay

(MTS, Promega) assays were performed as described to determine change in viable cell mass [32]. Cells were dissociated and seeded into 96-well plates at a density of 5,000 per well in 200 μl of medium and treated with DMSO or 1–50 nM TAK228, and incubated in 5% CO_2 at 37C. For the plate readings, 20 μl of MTS solution was added to each well after

at 0, 2, 5 and 7 days post-plating and incubated for 1 hour protected from light. The optical density at 490 nm was subsequently measured by spectrophotometer.

2.4 Cell proliferation assay

Proliferative ability was evaluated by using Bromodeoxyuridine (BrdU) as described previously [33]. Cells were treated with DMSO or 25 nM TAK228 for 3 days. BrdU (Sigma-Aldrich) was added 6 hours before collection. The collected neurospheres were triturated into single cells by Accutase, washed with PBS, fixed in cytospin fluid, and cytospun onto positively charged slides. BrdU (Sigma Aldrich) incorporation was measured as previously described [34].

2.5 Apoptosis assay

Apoptosis was evaluated by immunofluorescence of Cleaved Caspase 3 (CC3) as described previously [33]. Human DIPG cells were treated with DMSO or 25 nM TAK228 for 3 days. Murine PKC DIPG model cells were treated with 25 nM TAK228 for 2 days. The treated neurospheres were triturated into single cells, washed with PBS, fixed in cytospin fluid, and cytospun onto positively charged slides. Cells were then processed for CC3 detection using an anti-CC3 antibody (Asp175, Cell Signaling Technology) as described [35].

2.6 Combination therapy using TAK228 and Radiation

DIPG cells were treated with DMSO or 25 nM TAK228, and radiated with 2 Gy. Cells were exposed to radiation 4 hours after administration of TAK228, when p-AKT^{S473} was expected to be most inhibited, because of reports showing AKT inhibition enhancing radiosensitization [36; 37; 38]. Cells were incubated in TAK228 for an additional 72 hours before measuring proliferation and apoptosis using CC3 and BrdU, respectively. For mechanistic studies, cells were treated with 2 Gy radiation four hours after being placed in 25 nM TAK228. Cells were incubated in TAK228 for an additional 24 hours after radiation, at which time cells were harvested for western blotting. We chose this early timepoint to capture the events occurring upstream of the induction of apoptosis.

2.7 Invasion and migration assays

DIPG neurospheres were dissociated into single cells, re-suspended in media without both EGF and FGF, seeded at a density of 100,000 cells per trans-well insert (coated with Matrigel), and treated with DMSO or TAK228 as described previously [39; 40]. To minimize a direct cytotoxic effect of TAK228, the minimum dose of TAK228 that produced growth inhibition (10 nM) was selected. Regular EF media with DMSO or 10 nM TAK228 was added to the bottom of the trans-well to act as a chemoattractant. After incubation for 24 hours, cells that had moved to the bottom chamber of the trans-well insert were stained by hematoxylin and counted as described [39; 40].

Murine PKC neurospheres were grown in DMEM supplemented with 10% FBS and antibiotics for 24 h to form an adherent monolayer. Cells were then serum starved for 6 h. Cell monolayer was scraped in a straight line with a P200 pipet tip and washed with PBS to rinse away any floating cells. Cells were then treated with either vehicle or 25 nM TAK228 in complete DMEM media and imaged using 10 × objective at 0 h, 48 h and 6 days. The

scratch area was measured using Image J software. Percentage of wound closure was calculated as follows:

% Wound closure = $(A_{t = 0\ h} - A_{t = \Delta\ h})/A_{t = 0\ h} \times 100\%$, as described previously [41; 42; 43], where, $A_{t = 0\ h}$ is the area of the wound measured immediately after scratching and $A_{t = \Delta\ h}$ is the wound area measured at specific time interval after scratching.

2.8 Statistical analyses

Experiments were repeated at least 3 times in each cell line, unless otherwise noted. Statistical significance was evaluated using Student's *t*-test, unless otherwise noted. *P* values less than 0.05 were considered statistically significant. Error bars represent standard error of means unless otherwise stated. All statistical tests were performed using the GraphPad Prism 6 software (GraphPad Software, La Jolla, CA).

2.9 Establishment of DIPG orthotopic murine models

All mice work was performed in accordance with CNHS-IACUC approved protocol 30425. NOD SCID gamma mice (Age 3 wks, n=12) were used for orthotopic injection of PKC-L mouse neurospheres [29; 42]. Mice were anaesthetized using an isofluorane vaporizer and placed on a stereotactic frame fitted with a 26-gauge needle gas tight Hamilton syringe. After sterilizing the area, a 5 mm linear skin incision was made on the head to expose the skull. After determining the injection site in pons (2 mm posterior to the λ-suture, 1mM lateral to midline and 3 mm deep), a burr hole was made and a total of 300,000 live tumor neurospheres in 2 μl volume were injected [42]. Skin incision was sutured and mice were treated for pain with Buprenex (0.1 mg/kg) before returned to their home cages.

2.10 *In vivo* treatment with TAK228

Mice injected with tumor cells were divided into two groups (n=6 per group) to administer with vehicle or TAK228 (1 mg/kg, oral, Monday-Friday) starting from 7 days post injection with tumor cells. Tumor formation was confirmed by *in vivo* imaging for luciferase expression using IVIS Lumina III imaging system. Both groups were monitored daily for sickness and signs of tumor development including ataxia and weakness. When a mouse became sick, it was euthanized by CO_2 asphyxiation and the brain was harvested for histopathological analyses. Median survival differences between the two groups of mice were assessed using the log-rank test and visualized using Kaplan-Meier survival curve.

3. Results

3.1 TAK228 inhibited mTOR pathway activity in DIPG cells

To assess mTOR inhibition *in vitro* human primary DIPG cells (JHH-DIPG1, SF7761, SU-DIPG-XIII) were expanded in culture and exposed to TAK228 or vehicle control. mTOR pathway activity was assessed by western blot to measure levels of p-AKT^{S473}, total AKT, p-S6$^{S240/244}$, and total S6. Both p-AKT^{S473} and p-S6$^{S240/244}$ were highly expressed in DIPG cell lines and were inhibited between 50 to 90 percent after 4-hour-treatment with 25 nM TAK228 (Fig. 1A).

3.2 TAK228 suppressed the growth and proliferation of DIPG cells

DIPG neurospheres treated with TAK228 formed only small spheres as compared to DMSO (Fig. 1B). Cell growth of 3 DIPG cell lines as measured by MTS assay was inhibited by 10–50 nM TAK228 compared to DMSO (Fig. 1C; JHH-DIPG1: $p = 0.0021$ in 10 nM, $p = 0.0001$ in 25 nM, $p < 0.0001$ in 50 nM; SF7761: $p = 0.0002$ in 10 nM, $p < 0.0001$ in 25 and 50 nM; SU-DIPG-XIII: $p = 0.0065$ in 25 nM, $p = 0.0003$ in 50 nM).

To determine the effects of TAK228 on proliferation in DIPG cell lines, the percentage of BrdU-positive cells was assessed. An approximately 30% decrease of BrdU+ cells was seen after treatment with 25 nM TAK228 compared to DMSO control (Fig. 2A, B; JHH-DIPG1: 50.2% vs. 36.9%, $p < 0.0001$; SF7761: 49.1% vs. 32.0%, $p < 0.0001$; SU-DIPG-XIII: 44.4% vs. 31.9%, $p < 0.0001$; DMSO vs. TAK228).

3.3 TAK228 induced apoptosis in DIPG cells

Since apoptosis is known to be regulated by both mTORC1 and mTORC2 [44], we hypothesized that treatment with TAK228 would induce robust apoptosis. We measured apoptosis by cleaved caspase 3 (CC3) immunofluorescence after treatment with 25 nM TAK228. The percentage of CC3+ cells was significantly higher in the treatment group compared to DMSO control for each DIPG line (Fig. 3A, B; JHH-DIPG1: 2.4% vs. 6.1%, $p < 0.0001$; SF7761: 1.6% vs. 4.4%, $p = 0.0002$; SU-DIPG-XIII: 1.8% vs. 5.2%, $p < 0.0001$; DMSO vs. TAK228).

3.4 Combination of TAK228 and radiation enhanced apoptosis and suppressed proliferation

Radiation is one of the mainstays of DIPG treatment [1]. Since inhibition of AKT can enhance the cytotoxic effect of radiation [36; 37; 38], we hypothesized that treatment of DIPG with TAK228 would sensitize them to radiation. Combination of TAK228 and radiation enhanced the cytotoxic effects of radiation by suppressing proliferation (Fig. 2A, B; JHH-DIPG1: 36.5% vs. 26.0%, $p < 0.0001$; SF7761: 34.8% vs. 20.7%, $p < 0.0001$; SU-DIPG-XIII: 31.7% vs. 21.0%, $p < 0.0001$; radiation vs. combination) and inducing apoptosis (Fig. 3A, B; JHH-DIPG1: 7.3% vs. 12.4%, $p < 0.0001$; SF7761: 5.1% vs. 12.2%, $p = 0.0010$; SU-DIPG-XIII: 4.4% vs. 7.9%, $p = 0.0010$; radiation vs. combination).

To investigate the mechanism of how TAK228 enhanced the effect of radiation, we examined the expression of the anti-apoptotic proteins BCL-2 and BCL-XL after treatment with TAK228 and radiation. We found that in JHH DIPG1 and SF7761 there was a reproducible down-regulation of both BCL-2 and BCL-XL as measured by western blot with combination therapy (Figure 3C). This decrease in BCL-2 and BCL-XL was not observed reproducibly in SU-DIPG-XIII.

3.5 Low-dose TAK228 suppressed invasion

Invasion is also regulated by both mTORC1 and mTORC2 [45; 46; 47; 48; 49]. TAK228 treatment at 10 nM decreased invading cells in a Boyden matrigel transwell chamber assay by approximately 80% compared to DMSO in both SU-DIPG-XIII and JHH DIPG1 ($p<0.0001$ vs DMSO control) (Fig. 4A, B).

3.6 TAK228 inhibited tumor formation in an orthotopic DIPG murine model

Due to the long latency of tumor formation with human DIPG cell lines [26; 27], we assessed the efficacy of TAK228 *in vivo* using a well-established murine orthotopic DIPG model [29]. We first determined that TAK228 inhibited pAKT473 and pS6 at similar doses in these cells as in human DIPG cell line (Figure 5A). We then verified that the *in vitro* IC50 for this model was similar to that of human DIPG cells (Figure 5B). Treatment of the murine DIPG cells with 25 nM TAK228 led to induction of apoptosis as measured by CC3 immunofluorescence ($p<0.0001$ vs DMSO control) (Figure 5C, Supplemental Figure 1). TAK228 also suppressed murine DIPG cell migration when measured on days 2 and 6 of treatment ($p< 0.0001$ at both time points vs DMSO control) (Figure 5D, Supplemental Figure 2).

Orthotopic injection of murine DIPG cells expressing luciferase (PKC-L) into the pons of NOD SCID gamma mice (n=12) resulted in tumor growth within 10 days of transplantation, as visualized by *in vivo* imaging of luciferase activity. Mice were randomly assigned to treated (n=6) or control vehicle treated (n=6) groups. TAK228 treatment was begun starting 7 days after tumor cell injection at the generally accepted *in vivo* murine dose of 1 mg/kg orally, given Monday-Friday [50]. Mice tolerated this regimen well, without significant weight loss or other side effects. Survival analysis showed a more than doubling of the median survival of TAK228 treated mice as compared to vehicle treated, control mice (48 vs 101 days, Figure 5C $p=0.0017$ by Log-rank test).

4. Discussion

Inhibition of the mTOR pathway may represent an important treatment strategy in cancer. Although TORC1 inhibition with rapalogs did not show significant effect in a drug screen against DIPG cell lines [17], the activation of both mTORC1 and mTORC2 in DIPG suggests that dual mTORC kinase inhibitors may have increased potency in this tumor.

TAK228 is expected to promote apoptosis in DIPG because apoptosis is regulated by both mTORC1 and mTORC2 [51]. Meanwhile, multiple pro-invasion genes downstream of mTORC1 and mTORC2 are associated with metastasis in breast cancer [46; 48; 49], hepatocellular carcinoma [45; 52], and melanoma [47]. Furthermore, mTORC2, like mTORC1, is known to regulate cell growth through MYC activation [53]. Since apoptosis, invasion, and cell growth are governed by both mTORC1 and mTORC2, we hypothesized and showed that TAK228 induced apoptosis, suppressed invasion and inhibited cell growth.

Radiation is a standard treatment for DIPG, and a chemotherapeutic regimen showing radiosensitization is desired. In other cancer types, the combination of radiation and an AKT inhibitor enhanced apoptosis and DNA damage, and suppressed proliferation and clonogenicity [36; 37; 38]. In our study, combination with TAK228 and radiation also produced combinatorial efficacy.

We identified reproducible downregulation of the anti-apoptotic proteins BCL-2 and BCL-XL in JHH DIPG1 and SF7761 after treatment with TAK228 and 2Gy of radiation. SU-DIPG-XIII did not show reproducible reduction in BCL-2 and BCL-XL. In concordance

with a maintenance of robust expression of anti-apoptotic machinery, SU-DIPG-XIII also demonstrated the least induction of apoptosis after exposure to TAK228 and radiation.

In our *in vivo* experiments, TAK228 given daily at 1 mg/kg 5 days per week led to a significant increase in survival in a murine orthotopic DIPG model. Alternative dosing schedules have been reported in mice and humans that might allow a higher level of penetration into the brain. Some investigators have used a high dose, intermittent schedule of TAK228 in mice (3mg/kg twice daily for 3 days/week), which was tolerable and without harmful effects such as weight loss [22]. In humans, clinical trials are on-going in adult patients using different dosing schedules, including once-weekly doses of up to 30 mg (NCT02575339). The MTD and optimum dosing schedule of TAK228 in pediatric brain tumor patients has not yet been determined. Our data suggests that a phase I study in pediatric brain tumor patients may be reasonable.

In DIPG cell lines, the mTOR pathway is active, and inhibition of the pathway suppresses cell growth, proliferation, invasion, and induces apoptosis. These results may be a consequence of inhibition of both mTORC1 and mTORC2. Moreover, combination with radiation could enhance the therapeutic effects of TAK228 such as induction of apoptosis and suppression of proliferation. We conclude that dual mTOR inhibition is a promising candidate for DIPG treatment.

Supplementary Material

Refer to Web version on PubMed Central for supplementary material.

Acknowledgments

The authors thank Antoinette Price for excellent technical assistance. The SF7761 and SU-DIPG-XIII cell lines are kind gifts from Drs. Rintaro Hashizume and Michelle Monje, respectively.

Funding

Funding was provided by the Cure Starts Now Foundation to the Mid-Atlantic DIPG consortium (Drs. Nazarian, Raabe, Warren). Additional funding by the Giant Food Foundation, NCI Core Grant to the Johns Hopkins Sidney Kimmel Comprehensive Cancer Center P30 CA006973, Smashing Walnuts/Piedmont community (Dr. Nazarian), and the Goldwin Foundation (Dr. Nazarian). EHR is a St. Baldrick's Scholar.

References

1. Warren KE. Diffuse intrinsic pontine glioma: poised for progress. Front Oncol. 2012; 2:205. [PubMed: 23293772]
2. Buczkowicz P, Bartels U, Bouffet E, Becher O, Hawkins C. Histopathological spectrum of paediatric diffuse intrinsic pontine glioma: diagnostic and therapeutic implications. Acta Neuropathol. 2014; 128:573–581. [PubMed: 25047029]
3. Gielen GH, Gessi M, Hammes J, Kramm CM, Waha A, Pietsch T. H3F3A K27M mutation in pediatric CNS tumors: a marker for diffuse high-grade astrocytomas. Am J Clin Pathol. 2013; 139:345–349. [PubMed: 23429371]
4. Kallappagoudar S, Yadav RK, Lowe BR, Partridge JF. Histone H3 mutations-a special role for H3.3 in tumorigenesis? Chromosoma. 2015; 124:177–189. [PubMed: 25773741]
5. Khuong-Quang DA, Buczkowicz P, Rakopoulos P, Liu XY, Fontebasso AM, Bouffet E, Bartels U, Albrecht S, Schwartzentruber J, Letourneau L, Bourgey M, Bourque G, Montpetit A, Bourret G, Lepage P, Fleming A, Lichter P, Kool M, von Deimling A, Sturm D, Korshunov A, Faury D, Jones

DT, Majewski J, Pfister SM, Jabado N, Hawkins C. K27M mutation in histone H3.3 defines clinically and biologically distinct subgroups of pediatric diffuse intrinsic pontine gliomas. Acta Neuropathol. 2012; 124:439–447. [PubMed: 22661320]

6. Hoffman LM, DeWire M, Ryall S, Buczkowicz P, Leach J, Miles L, Ramani A, Brudno M, Kumar SS, Drissi R, Dexheimer P, Salloum R, Chow L, Hummel T, Stevenson C, Lu QR, Jones B, Witte D, Aronow B, Hawkins CE, Fouladi M. Spatial genomic heterogeneity in diffuse intrinsic pontine and midline high-grade glioma: implications for diagnostic biopsy and targeted therapeutics. Acta Neuropathol Commun. 2016; 4:1. [PubMed: 26727948]
7. Nikbakht H, Panditharatna E, Mikael LG, Li R, Gayden T, Osmond M, Ho CY, Kambhampati M, Hwang EI, Faury D, Siu A, Papillon-Cavanagh S, Bechet D, Ligon KL, Ellezam B, Ingram WJ, Stinson C, Moore AS, Warren KE, Karamchandani J, Packer RJ, Jabado N, Majewski J, Nazarian J. Spatial and temporal homogeneity of driver mutations in diffuse intrinsic pontine glioma. Nature communications. 2016; 7:11185.
8. Buczkowicz P, Hoeman C, Rakopoulos P, Pajovic S, Letourneau L, Dzamba M, Morrison A, Lewis P, Bouffet E, Bartels U, Zuccaro J, Agnihotri S, Ryall S, Barszczyk M, Chornenkyy Y, Bourgey M, Bourque G, Montpetit A, Cordero F, Castelo-Branco P, Mangerel J, Tabori U, Ho KC, Huang A, Taylor KR, Mackay A, Bendel AE, Nazarian J, Fangusaro JR, Karajannis MA, Zagzag D, Foreman NK, Donson A, Hegert JV, Smith A, Chan J, Lafay-Cousin L, Dunn S, Hukin J, Dunham C, Scheinemann K, Michaud J, Zelcer S, Ramsay D, Cain J, Brennan C, Souweidane MM, Jones C, Allis CD, Brudno M, Becher O, Hawkins C. Genomic analysis of diffuse intrinsic pontine gliomas identifies three molecular subgroups and recurrent activating ACVR1 mutations. Nat Genet. 2014; 46:451–456. [PubMed: 24705254]
9. Warren KE, Killian K, Suuriniemi M, Wang Y, Quezado M, Meltzer PS. Genomic aberrations in pediatric diffuse intrinsic pontine gliomas. Neuro Oncol. 2012; 14:326–332. [PubMed: 22064882]
10. Zarghooni M, Bartels U, Lee E, Buczkowicz P, Morrison A, Huang A, Bouffet E, Hawkins C. Whole-Genome Profiling of Pediatric Diffuse Intrinsic Pontine Gliomas Highlights Platelet-Derived Growth Factor Receptor {alpha} and Poly (ADP-ribose) Polymerase As Potential Therapeutic Targets. J Clin Oncol. 2010
11. Puget S, Beccaria K, Blauwblomme T, Roujeau T, James S, Grill J, Zerah M, Varlet P, Sainte-Rose C. Biopsy in a series of 130 pediatric diffuse intrinsic Pontine gliomas. Child's nervous system : ChNS : official journal of the International Society for Pediatric Neurosurgery. 2015; 31:1773–1780.
12. Laplante M, Sabatini DM. mTOR signaling in growth control and disease. Cell. 2012; 149:274–293. [PubMed: 22500797]
13. Heikamp EB, Patel CH, Collins S, Waickman A, Oh MH, Sun IH, Illei P, Sharma A, Naray-Fejes-Toth A, Fejes-Toth G, Misra-Sen J, Horton MR, Powell JD. The AGC kinase SGK1 regulates TH1 and TH2 differentiation downstream of the mTORC2 complex. Nat Immunol. 2014; 15:457–464. [PubMed: 24705297]
14. Rispal D, Eltschinger S, Stahl M, Vaga S, Bodenmiller B, Abraham Y, Filipuzzi I, Movva NR, Aebersold R, Helliwell SB, Loewith R. Target of Rapamycin Complex 2 Regulates Actin Polarization and Endocytosis via Multiple Pathways. J Biol Chem. 2015; 290:14963–14978. [PubMed: 25882841]
15. Zarghooni M, Bartels U, Lee E, Buczkowicz P, Morrison A, Huang A, Bouffet E, Hawkins C. Whole-genome profiling of pediatric diffuse intrinsic pontine gliomas highlights platelet-derived growth factor receptor alpha and poly (ADP-ribose) polymerase as potential therapeutic targets. J Clin Oncol. 2010; 28:1337–1344. [PubMed: 20142589]
16. Schenone S, Brullo C, Musumeci F, Radi M, Botta M. ATP-competitive inhibitors of mTOR: an update. Curr Med Chem. 2011; 18:2995–3014. [PubMed: 21651476]
17. Grasso CS, Tang Y, Truffaux N, Berlow NE, Liu L, Debily M-A, Quist MJ, Davis LE, Huang EC, Woo PJ, Ponnuswami A, Chen S, Johung TB, Sun W, Kogiso M, Du Y, Qi L, Huang Y, Hutt-Cabezas M, Warren KE, Le Dret L, Meltzer PS, Mao H, Quezado M, van Vuurden DG, Abraham J, Fouladi M, Svalina MN, Wang N, Hawkins C, Nazarian J, Alonso MM, Raabe EH, Hulleman E, Spellman PT, Li X-N, Keller C, Pal R, Grill J, Monje M. Functionally defined therapeutic targets in diffuse intrinsic pontine glioma. Nat Med advance online publication. 2015

18. Guertin DA, Sabatini DM. The pharmacology of mTOR inhibition. Sci Signal. 2009; 2:pe24. [PubMed: 19383975]
19. Hassan B, Akcakanat A, Sangai T, Evans KW, Adkins F, Eterovic AK, Zhao H, Chen K, Chen H, Do KA, Xie SM, Holder AM, Naing A, Mills GB, Meric-Bernstam F. Catalytic mTOR inhibitors can overcome intrinsic and acquired resistance to allosteric mTOR inhibitors. Oncotarget. 2014; 5:8544–8557. [PubMed: 25261369]
20. Hsieh AC, Liu Y, Edlind MP, Ingolia NT, Janes MR, Sher A, Shi EY, Stumpf CR, Christensen C, Bonham MJ, Wang S, Ren P, Martin M, Jessen K, Feldman ME, Weissman JS, Shokat KM, Rommel C, Ruggero D. The translational landscape of mTOR signalling steers cancer initiation and metastasis. Nature. 2012; 485:55–61. [PubMed: 22367541]
21. Garcia-Garcia C, Ibrahim YH, Serra V, Calvo MT, Guzman M, Grueso J, Aura C, Perez J, Jessen K, Liu Y, Rommel C, Tabernero J, Baselga J, Scaltriti M. Dual mTORC1/2 and HER2 blockade results in antitumor activity in preclinical models of breast cancer resistant to anti-HER2 therapy. Clin Cancer Res. 2012; 18:2603–2612. [PubMed: 22407832]
22. Slotkin EK, Patwardhan PP, Vasudeva SD, de Stanchina E, Tap WD, Schwartz GK. MLN0128, an ATP-competitive mTOR kinase inhibitor with potent in vitro and in vivo antitumor activity, as potential therapy for bone and soft-tissue sarcoma. Mol Cancer Ther. 2015; 14:395–406. [PubMed: 25519700]
23. Lou HZ, Weng XC, Pan HM, Pan Q, Sun P, Liu LL, Chen B. The novel mTORC1/2 dual inhibitor INK-128 suppresses survival and proliferation of primary and transformed human pancreatic cancer cells. Biochem Biophys Res Commun. 2014; 450:973–978. [PubMed: 24971544]
24. Zhang H, Dou J, Yu Y, Zhao Y, Fan Y, Cheng J, Xu X, Liu W, Guan S, Chen Z, shi Y, Patel R, Vasudevan SA, Zage PE, Zhang H, Nuchtern JG, Kim ES, Fu S, Yang J. mTOR ATP-competitive inhibitor INK128 inhibits neuroblastoma growth via blocking mTORC signaling. Apoptosis. 2015; 20:50–62. [PubMed: 25425103]
25. Gokmen-Polar Y, Liu Y, Toroni RA, Sanders KL, Mehta R, Badve S, Rommel C, Sledge GW Jr. Investigational drug MLN0128, a novel TORC1/2 inhibitor, demonstrates potent oral antitumor activity in human breast cancer xenograft models. Breast Cancer Res Treat. 2012; 136:673–682. [PubMed: 23085766]
26. Taylor IC, Hutt-Cabezas M, Brandt WD, Kambhampati M, Nazarian J, Chang HT, Warren KE, Eberhart CG, Raabe EH. Disrupting NOTCH Slows Diffuse Intrinsic Pontine Glioma Growth, Enhances Radiation Sensitivity, and Shows Combinatorial Efficacy With Bromodomain Inhibition. Journal of neuropathology and experimental neurology. 2015; 74:778–790. [PubMed: 26115193]
27. Hashizume R, Smirnov I, Liu S, Phillips JJ, Hyer J, McKnight TR, Wendland M, Prados M, Banerjee A, Nicolaides T, Mueller S, James CD, Gupta N. Characterization of a diffuse intrinsic pontine glioma cell line: implications for future investigations and treatment. J Neurooncol. 2012; 110:305–313. [PubMed: 22983601]
28. Grasso CS, Tang Y, Truffaux N, Berlow NE, Liu L, Debily MA, Quist MJ, Davis LE, Huang EC, Woo PJ, Ponnuswami A, Chen S, Johung TB, Sun W, Kogiso M, Du Y, Qi L, Huang Y, Hutt-Cabezas M, Warren KE, Le Dret L, Meltzer PS, Mao H, Quezado M, van Vuurden DG, Abraham J, Fouladi M, Svalina MN, Wang N, Hawkins C, Nazarian J, Alonso MM, Raabe EH, Hulleman E, Spellman PT, Li XN, Keller C, Pal R, Grill J, Monje M. Erratum: Functionally defined therapeutic targets in diffuse intrinsic pontine glioma. Nat Med. 2015; 21:827.
29. Halvorson KG, Barton KL, Schroeder K, Misuraca KL, Hoeman C, Chung A, Crabtree DM, Cordero FJ, Singh R, Spasojevic I, Berlow N, Pal R, Becher OJ. A high-throughput in vitro drug screen in a genetically engineered mouse model of diffuse intrinsic pontine glioma identifies BMS-754807 as a promising therapeutic agent. PLoS One. 2015; 10:e0118926. [PubMed: 25748921]
30. Hutt-Cabezas M, Karajannis MA, Zagzag D, Shah S, Horkayne-Szakaly I, Rushing EJ, Cameron JD, Jain D, Eberhart CG, Raabe EH, Rodriguez FJ. Activation of mTORC1/mTORC2 signaling in pediatric low-grade glioma and pilocytic astrocytoma reveals mTOR as a therapeutic target. Neuro-oncology. 2013; 15:1604–1614. [PubMed: 24203892]
31. Rasband, WS. ImageJ. U.S. National Institutes of Health; Bethesda, Maryland, USA: p. 1997-2016.

32. Mao XG, Hutt-Cabezas M, Orr BA, Weingart M, Taylor I, Rajan AK, Odia Y, Kahlert U, Maciaczyk J, Nikkhah G, Eberhart CG, Raabe EH. LIN28A facilitates the transformation of human neural stem cells and promotes glioblastoma tumorigenesis through a pro-invasive genetic program. Oncotarget. 2013; 4:1050–1064. [PubMed: 23846349]

33. Weingart MF, Roth JJ, Hutt-Cabezas M, Busse TM, Kaur H, Price A, Maynard R, Rubens J, Taylor I, Mao XG, Xu J, Kuwahara Y, Allen SJ, Erdreich-Epstein A, Weissman BE, Orr BA, Eberhart CG, Biegel JA, Raabe EH. Disrupting LIN28 in atypical teratoid rhabdoid tumors reveals the importance of the mitogen activated protein kinase pathway as a therapeutic target. Oncotarget. 2014

34. Raabe EH, Lim KS, Kim JM, Meeker A, Mao XG, Nikkhah G, Maciaczyk J, Kahlert U, Jain D, Bar E, Cohen KJ, Eberhart CG. BRAF activation induces transformation and then senescence in human neural stem cells: a pilocytic astrocytoma model. Clin Cancer Res. 2011; 17:3590–3599. [PubMed: 21636552]

35. Weingart MF, Roth JJ, Hutt-Cabezas M, Busse TM, Kaur H, Price A, Maynard R, Rubens J, Taylor I, Mao XG, Xu J, Kuwahara Y, Allen SJ, Erdreich-Epstein A, Weissman BE, Orr BA, Eberhart CG, Biegel JA, Raabe EH. Disrupting LIN28 in atypical teratoid rhabdoid tumors reveals the importance of the mitogen activated protein kinase pathway as a therapeutic target. Oncotarget. 2015; 6:3165–3177. [PubMed: 25638158]

36. Choi EJ, Cho BJ, Lee DJ, Hwang YH, Chun SH, Kim HH, Kim IA. Enhanced cytotoxic effect of radiation and temozolomide in malignant glioma cells: targeting PI3K-AKT-mTOR signaling, HSP90 and histone deacetylases. BMC Cancer. 2014; 14:17. [PubMed: 24418474]

37. Mehta M, Khan A, Danish S, Haffty BG, Sabaawy HE. Radiosensitization of Primary Human Glioblastoma Stem-like Cells with Low-Dose AKT Inhibition. Mol Cancer Ther. 2015; 14:1171–1180. [PubMed: 25695954]

38. Millet P, Granotier C, Etienne O, Boussin FD. Radiation-induced upregulation of telomerase activity escapes PI3-kinase inhibition in two malignant glioma cell lines. Int J Oncol. 2013; 43:375–382. [PubMed: 23727752]

39. Kaur H, Hutt-Cabezas M, Weingart MF, Xu J, Kuwahara Y, Erdreich-Epstein A, Weissman BE, Eberhart CG, Raabe EH. The Chromatin-Modifying Protein HMGA2 Promotes Atypical Teratoid/Rhabdoid Cell Tumorigenicity. Journal of neuropathology and experimental neurology. 2015; 74:177–185. [PubMed: 25575139]

40. Kaur H, Ali SZ, Huey L, Hutt-Cabezas M, Taylor I, Mao XG, Weingart M, Chu Q, Rodriguez FJ, Eberhart CG, Raabe EH. The transcriptional modulator HMGA2 promotes stemness and tumorigenicity in glioblastoma. Cancer Lett. 2016; 377:55–64. [PubMed: 27102002]

41. Kaur H, Phillips-Mason PJ, Burden-Gulley SM, Kerstetter-Fogle AE, Basilion JP, Sloan AE, Brady-Kalnay SM. Cadherin-11, a marker of the mesenchymal phenotype, regulates glioblastoma cell migration and survival in vivo. Molecular cancer research : MCR. 2012; 10:293–304. [PubMed: 22267545]

42. Yadavilli S, Scafidi J, Becher OJ, Saratsis AM, Hiner RL, Kambhampati M, Mariarita S, MacDonald TJ, Codispoti KE, Magge SN, Jaiswal JK, Packer RJ, Nazarian J. The emerging role of NG2 in pediatric diffuse intrinsic pontine glioma. Oncotarget. 2015; 6:12141–12155. [PubMed: 25987129]

43. Yue PY, Leung EP, Mak NK, Wong RN. A simplified method for quantifying cell migration/wound healing in 96-well plates. J Biomol Screen. 2010; 15:427–433. [PubMed: 20208035]

44. Guertin DA, Sabatini DM. An expanding role for mTOR in cancer. Trends Mol Med. 2005; 11:353–361. [PubMed: 16002336]

45. Yang MY, Hsu LS, Peng CH, Shi YS, Wu CH, Wang CJ. Polyphenol-rich extracts from Solanum nigrum attenuated PKC alpha-mediated migration and invasion of hepatocellular carcinoma cells. J Agric Food Chem. 2010; 58:5806–5814. [PubMed: 20349911]

46. Noh EM, Lee YR, Hong OY, Jung SH, Youn HJ, Kim JS. Aurora kinases are essential for PKC-induced invasion and matrix metalloproteinase-9 expression in MCF-7 breast cancer cells. Oncol Rep. 2015

47. Matsuoka H, Tsubaki M, Yamazoe Y, Ogaki M, Satou T, Itoh T, Kusunoki T, Nishida S. Tamoxifen inhibits tumor cell invasion and metastasis in mouse melanoma through suppression of

PKC/MEK/ERK and PKC/PI3K/Akt pathways. Exp Cell Res. 2009; 315:2022–2032. [PubMed: 19393235]

48. Eun SY, Ko YS, Park SW, Chang KC, Kim HJ. P2Y2 nucleotide receptor-mediated extracellular signal-regulated kinases and protein kinase C activation induces the invasion of highly metastatic breast cancer cells. Oncol Rep. 2015; 34:195–202. [PubMed: 26063340]
49. Hou J, Wang Z, Xu H, Yang L, Yu X, Yang Z, Deng Y, Meng J, Feng Y, Guo X, Yang G. Stanniocalicin 2 suppresses breast cancer cell migration and invasion via the PKC/claudin-1-mediated signaling. PLoS One. 2015; 10:e0122179. [PubMed: 25830567]
50. Kang MH, Reynolds CP, Maris JM, Gorlick R, Kolb EA, Lock R, Carol H, Keir ST, Wu J, Lyalin D, Kurmasheva RT, Houghton PJ, Smith MA. Initial testing (stage 1) of the investigational mTOR kinase inhibitor MLN0128 by the pediatric preclinical testing program. Pediatric blood & cancer. 2014; 61:1486–1489. [PubMed: 24623675]
51. Mazan-Mamczarz K, Peroutka RJ, Steinhardt JJ, Gidoni M, Zhang Y, Lehrmann E, Landon AL, Dai B, Houng S, Muniandy PA, Efroni S, Becker KG, Gartenhaus RB. Distinct inhibitory effects on mTOR signaling by ethanol and INK128 in diffuse large B-cell lymphoma. Cell Commun Signal. 2015; 13:15. [PubMed: 25849580]
52. Masri J, Bernath A, Martin J, Jo OD, Vartanian R, Funk A, Gera J. mTORC2 activity is elevated in gliomas and promotes growth and cell motility via overexpression of rictor. Cancer Res. 2007; 67:11712–11720. [PubMed: 18089801]
53. Kuo Y, Huang H, Cai T, Wang T. Target of Rapamycin Complex 2 regulates cell growth via Myc in Drosophila. Sci Rep. 2015; 5:10339. [PubMed: 25999153]

Highlights

- TAK228 inhibited p-AKT and p-S6 in DIPG.
- TAK228 suppressed cell growth, proliferation, invasion, and induced apoptosis in DIPG.
- TAK228 acted as a radiosensitizer in DIPG.
- TAK228 treatment more than doubled the median survival of an orthotopic murine model of DIPG.

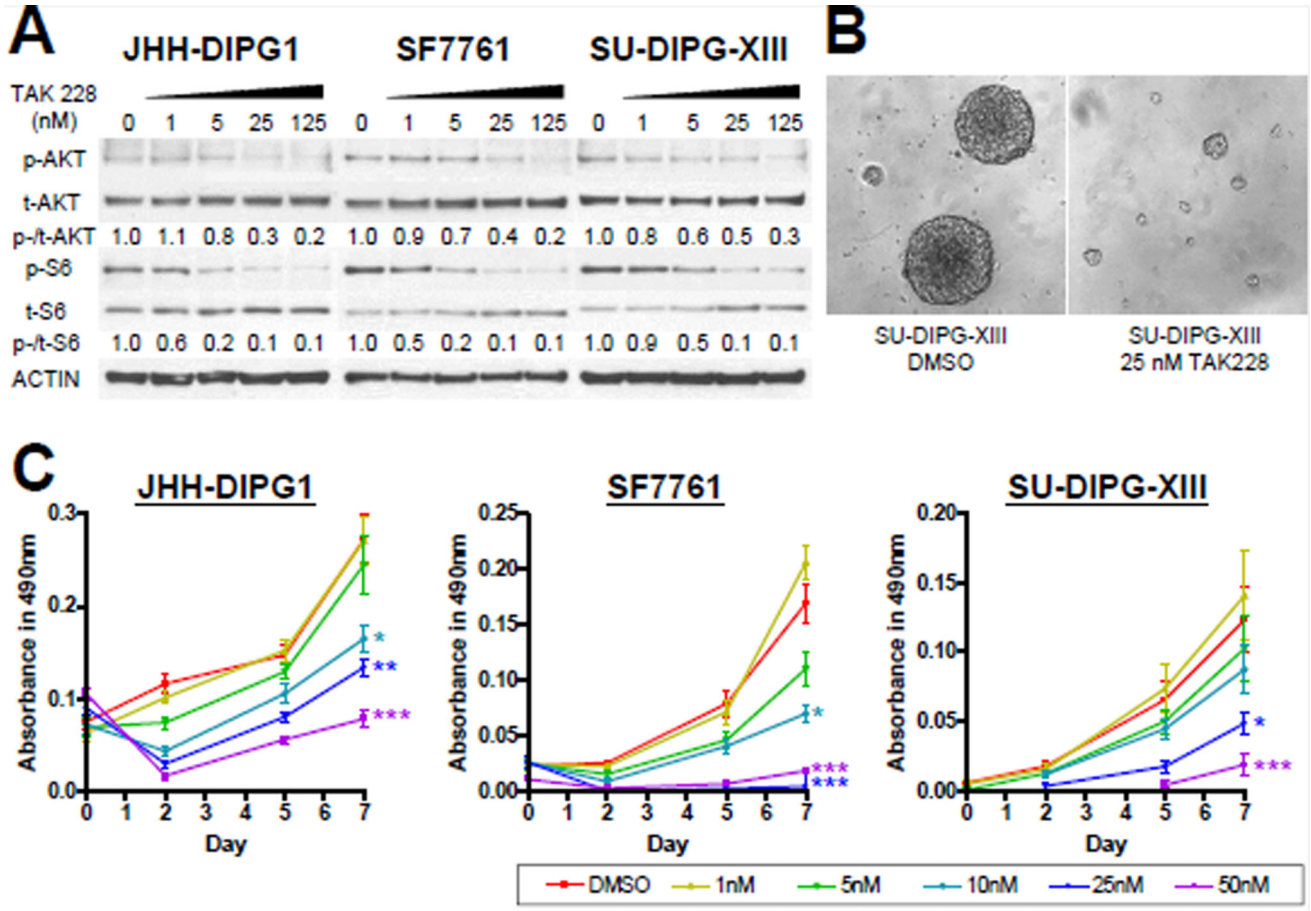

Figure 1. TAK228 inhibited mTOR pathway activity and suppressed cell growth in DIPG lines at nM concentrations

A) Western blot showing dose-dependent suppression of both p-AKT^{S473} and p-S6$^{S240/244}$ by TAK228. ACTIN was used as a loading control. Protein levels were quantitated using densitometry, and values normalized to DMSO control are depicted below the blots. B) High power (400X) photomicrograph comparing DIPG neurospheres of treated cells (right) as compared to control DMSO cells (left). C) MTS viability assay showing cell growth inhibition of all DIPG lines by 25–50 nM TAK228 compared to DMSO. ***: $p < 0.0001$, **: $p < 0.01$, *: $p < 0.05$ vs. DMSO by Student's t-test.

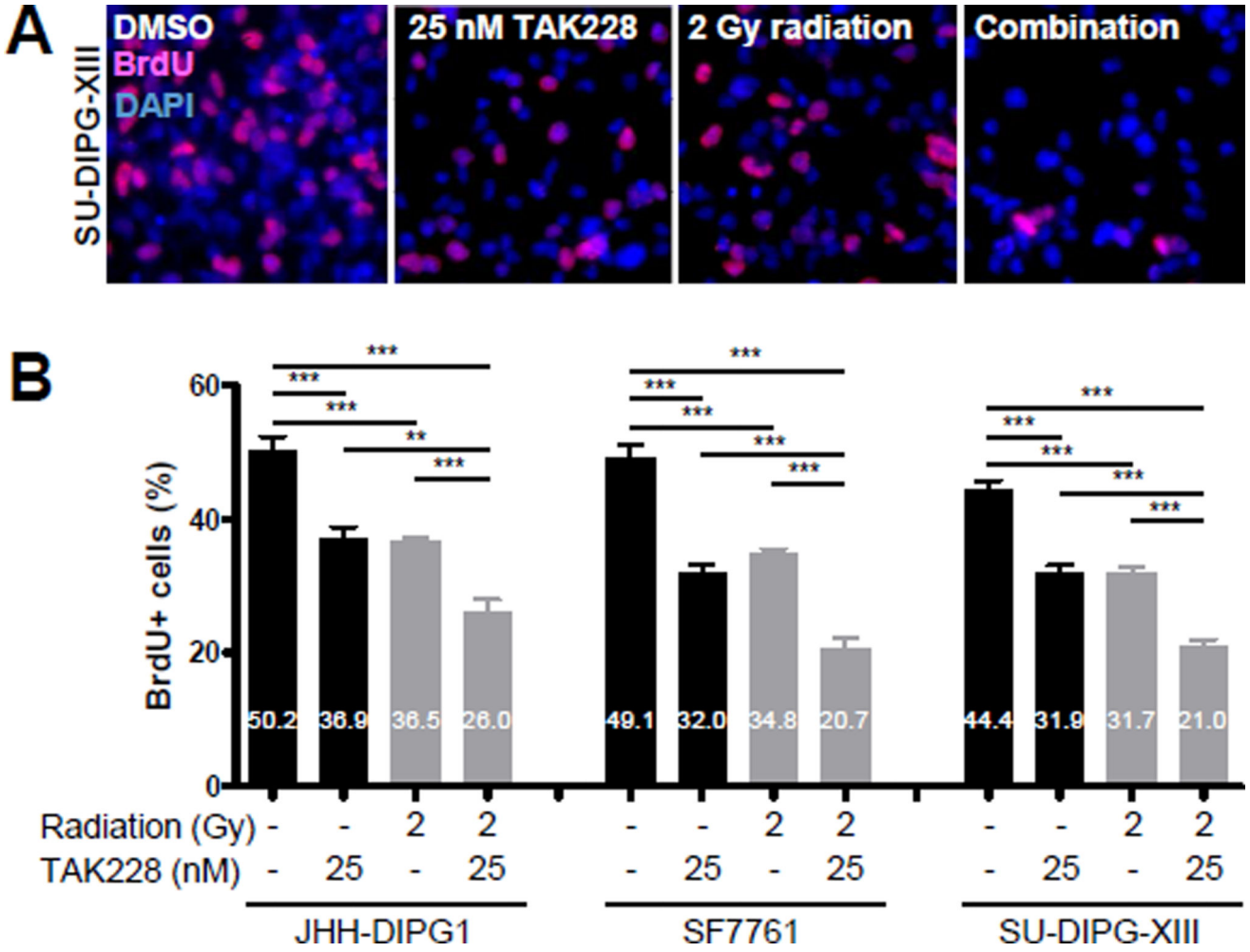

Figure 2.

TAK228 suppressed DIPG proliferation and enhanced radiosensitization

A) Representative 400× photomicrographs showing decreased proliferation as measured by BrdU immunofluorescence (red) after treatment with 25 nM TAK228 for 3 days followed by 2 Gy radiation. DAPI counterstains nuclei (blue). B) Quantification of DIPG proliferation after TAK228 and radiation treatment ***: $p < 0.0001$, **: $p < 0.01$, *: $p < 0.05$ vs. DMSO by t-test.

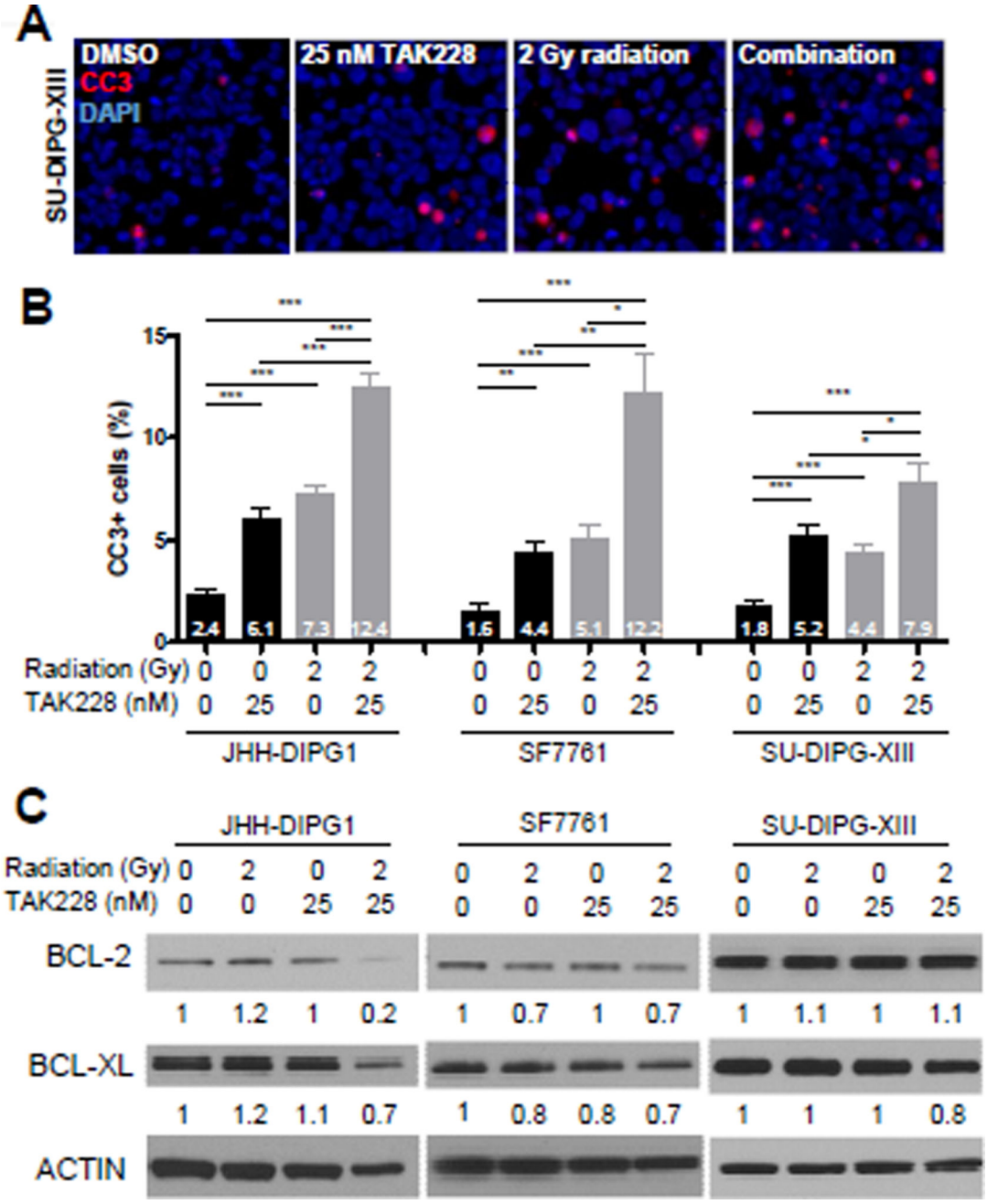

Figure 3. TAK228 induced apoptosis and enhanced radiotoxicity in DIPG

A) Representative 400× photomicrographs showing increased apoptosis after treatment with TAK228 and radiation. Four hours after placing cells in 25 nM TAK228, cells were irradiated with 2 Gy radiation. Cells were incubated with 25 nM TAK228 for an additional 72 hours and processed for immunofluorescence for CC3 (red). DAPI counterstains nuclei (blue). B) Percentage of CC3+ cells increased significantly after treatment with 25 nM TAK228, and further increased when combined with 2 Gy of radiation. ***: $p < 0.0001$, **: $p < 0.01$, *: $p < 0.05$ vs. DMSO by t-test. C) Western blot showing expression of BCL-2 and BCL-XL proteins in human DIPG after treatment with 25 nM TAK228 and 2 Gy radiation.

Cells were harvested 24 hours after radiation to capture early events leading to increased apoptosis. ACTIN was used as a loading control. Protein levels were quantitated using densitometry, and values normalized to DMSO control are depicted below the blots.

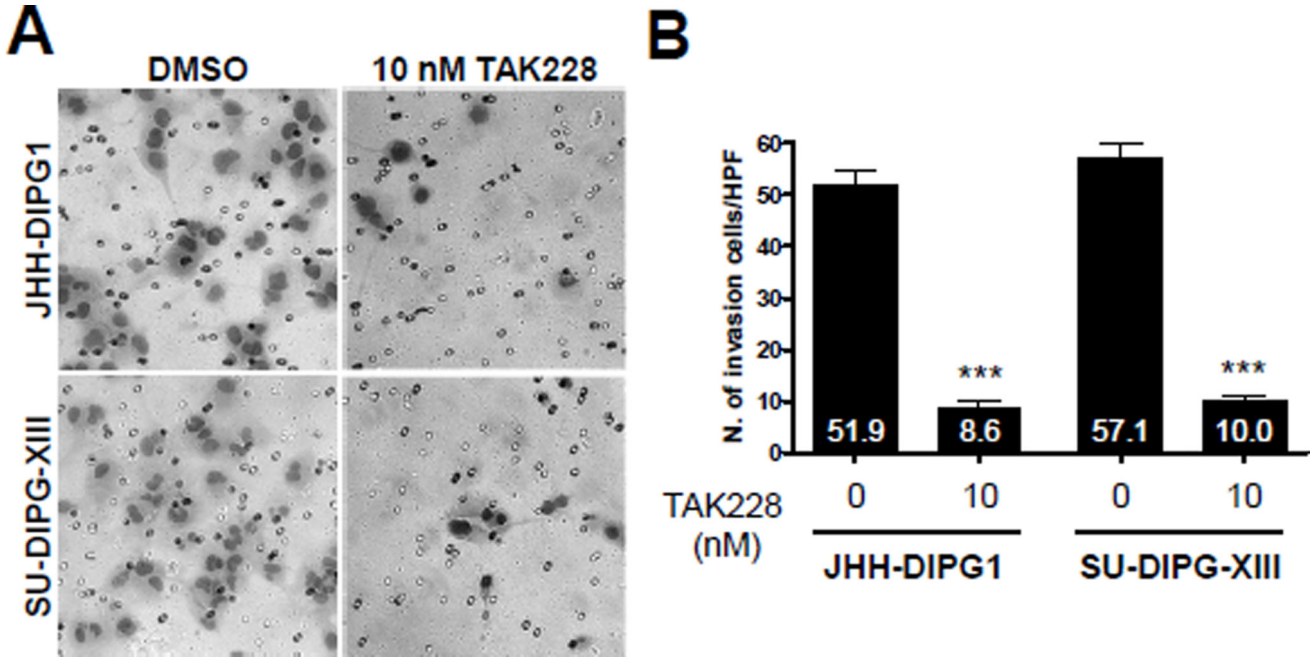

Figure 4.

TAK228 suppressed invasion in DIPG. A. High power images showing migrated cells in control and TAK228 treated cells. B. Quantification of number of migrating cells. *** indicates $p < 0.0001$ vs. DMSO by t-test.

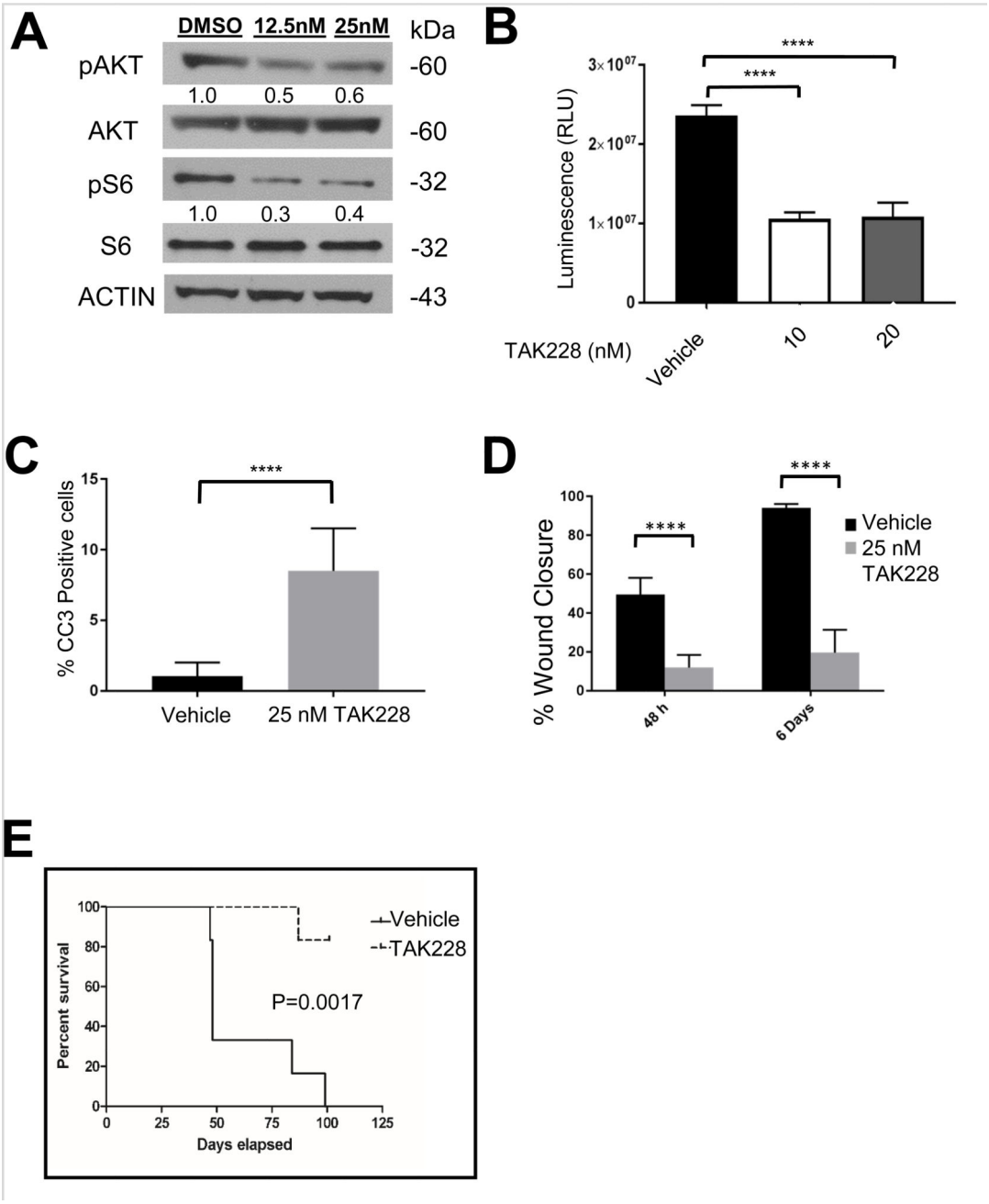

Figure 5. TAK228 inhibited pS6 and pAKT and suppressed growth and tumorigenicity of PKC-L murine DIPG neurospheres

A. Western blot showing TAK228 inhibition of pS6 and pAKT 473 in PKC-L murine DIPG cells. ACTIN was used as a loading control. Protein levels were quantitated using densitometry, and values normalized to DMSO control are depicted below the blots.

B. TAK228 suppressed the growth of PKC-L murine DIPG cells *in vitro* as measured by CytoTox-Glo cytotoxicity kit. PKC neurospheres were treated with vehicle, 10 or 20 nM of TAK228 for 7 days and luminescence from total cells in each sample was determined by using CytoTox-Glo cytotoxicity kit. Average of triplicate values of each sample were plotted. P value < 0.0001 as determined by one way Anova. Error bars: SD. C. Graph

showing quantification of percent apoptotic cells as measured by CC3 immunofluorescence in PKC-L cells. P value <0.0001 by t-test. D. Graph showing quantification of percent would closure after 2 and 6 days of treatment in 25 nM TAK228 compared to DMSO control. P value <0.0001 by t-test. E. Kaplan-Meier survival curve showing that TAK228 treatment extends the life of mice bearing orthotopic grafts of PKC-L DIPG neurosphere cells. P=0.0017 by log-rank test.